



# Development and Performance Evaluation of $WO_3/ZnO$ Composite Membranes for Antibiotics Wastewater Treatment

Muhammad Itsar Hanif Andri Cahyo Kumoro and Tutuk Djoko Kusworo\*

Chemical Engineering Diponegoro University, Semarang, Indonesia

Corresponding author Email: [tdkusworo@che.undip.ac.id](mailto:tdkusworo@che.undip.ac.id)

**Abstract** - The contamination of water resources with pharmaceutical pollutants, particularly tetracycline (TC), has become a pressing environmental issue. This poses a significant threat to ecosystems and public health, as untreated wastewater can lead to the spread of antibiotic resistance. In this study, we explore the potential of PVDF-based membranes integrated with  $WO_3/ZnO$  composites for effectively removing TC and COD from wastewater. Membranes with varying concentrations of  $WO_3/ZnO$  (0.25%, 0.75%, 1.25%) were evaluated in terms of flux, pollutant rejection efficiency, and pore properties. Among the tested membranes, MV-3 (PVDF neat 13% +  $WO_3/ZnO$  1.25%) demonstrated the best performance, achieving 98.28% rejection for TC and 87.72% for COD. Additionally, MV-3 exhibited the highest porosity (67.81%), although flux decreased moderately. This highlights the trade-off between high rejection efficiency and flux but demonstrates that the addition of  $WO_3/ZnO$  to PVDF membranes can provide a balanced solution for efficient wastewater treatment.

**Keywords** -PVDF,  $WO_3/ZnO$ , tetracycline removal, wastewater treatment, antibiotic removal.

**Doi:** <http://dx.doi.org/10.14710/wastech.14.1.8-15>

[How to cite this article: Hanif, M.I., Kumoro, A.C., Kusworo, T.D. (2026). Development and Performance Evaluation of  $WO_3/ZnO$  Composite Membranes for Antibiotics Wastewater Treatment, 14(1), 8-15 doi: <http://dx.doi.org/10.14710/wastech.14.1.8-15>]

## 1. Introduction

The widespread use of antibiotics has become a significant global health issue due to the growing problem of antibiotic-resistant bacteria (ARB). Antibiotic resistance develops when bacteria adapt and acquire mechanisms that allow them to survive treatments that would typically kill or inhibit their growth. One of the major contributors to this issue is the contamination of water sources through the discharge of wastewater from various industries, agriculture, and domestic use. Research indicates that many wastewater treatment facilities are not effective at removing these contaminants, leading to the spread of ARB into natural water systems (Frieri et al., 2017). Among the most commonly used antibiotics is tetracycline (TC), which is widely employed in both human medicine and agriculture, especially for treating livestock diseases and promoting growth. However, the substantial presence of TC in wastewater and natural water sources raises significant environmental concerns. When released into aquatic environments, TC residues accumulate, which can have harmful effects on aquatic organisms and pose risks to human populations dependent on these water sources for

consumption and recreation. As ARB continues to spread, the transmission of resistance genes becomes an alarming issue, with long-lasting consequences for human health, particularly in the treatment of infectious diseases (Carlet et al., 2014). The persistence of tetracycline in these systems is compounded by its poor biodegradability, presenting serious challenges to conventional wastewater treatment methods (Gaur et al., 2022).

Membrane technology has become widely recognized as one of the most effective techniques for wastewater treatment, owing to its capacity to separate pollutants based on their size and physical properties (Mirwan et al., 2017). Despite its advantages, a significant challenge that persists in membrane technology is membrane fouling. This phenomenon, which involves the buildup of organic and inorganic substances on the surface of the membrane, leads to a reduction in permeate flux and significantly shortens the membrane's service life. As a result, fouling contributes to increased operational costs and more frequent maintenance requirements (Mallah et al., 2024). To overcome these challenges, there is an increasing demand for photocatalytic membranes that not only serve as filters for pollutants but

also facilitate the degradation and transformation of contaminants via light activation, thus addressing fouling concerns during the treatment process (Kusworo et al., 2018).

A promising approach to improving membrane performance in wastewater treatment involves the use of composite photocatalytic membranes, which integrate semiconductor materials with membranes to enhance their photocatalytic capabilities (Ibrahim et al., 2025). This research specifically examines the combination of  $WO_3$  (Tungsten Trioxide) and ZnO (Zinc Oxide), both of which have demonstrated significant potential in photocatalytic applications.  $WO_3$ , with a band gap between 2.6 and 2.8 eV, can absorb both UV and some visible light, thereby enhancing its photocatalytic efficiency and minimizing electron-hole recombination, which in turn improves the stability and durability of the membrane (Yuju et al., 2023). However, the photocatalytic activity of  $WO_3$  is limited by the rapid recombination of electron-hole pairs. In contrast, ZnO, with a band gap of approximately 3.3 eV, boosts UV absorption and aids in charge separation, improving the membrane's conductivity and flux during filtration (Cifre-Herrando et al., 2023). The integration of  $WO_3$  and ZnO creates a heterojunction that facilitates efficient charge separation by enabling electron transfer from ZnO to  $WO_3$ , while keeping the holes in  $WO_3$ , thereby reducing recombination losses. This charge transfer mechanism increases carrier lifetime and enhances the generation of reactive oxygen species (ROS), which are crucial for the photocatalytic degradation of persistent pollutants like tetracycline (Sajjad et al., 2018). The incorporation of both  $WO_3$  and ZnO in composite membranes improves not only their photocatalytic activity but also their hydrophilicity, which reduces fouling and enhances overall filtration performance.

This study aims to assess the performance of  $WO_3$ /ZnO photocatalytic membranes in treating wastewater contaminated with tetracycline (TC) and COD. Specifically, the research will explore how effectively the  $WO_3$ /ZnO composite membrane can degrade TC and reduce the COD levels in wastewater, while also evaluating its impact on membrane flux and fouling resistance. Additionally, the study will involve tests for flux, rejection, and porosity to gauge the membrane's performance in terms of permeability, contaminant removal efficiency, and structural properties. The flux test will measure the membrane's ability to allow permeate flow and its potential for high performance filtration, while the rejection test will focus on its selective removal of contaminants, specifically TC and COD. The porosity test will help to determine how the membrane's structural characteristics affect its filtration efficiency, fouling resistance, and mass transfer, all of which are vital for optimizing membrane performance in wastewater treatment. The manuscript will also explore the mechanisms through which  $WO_3$  and ZnO enhance the photocatalytic efficiency of the membrane and provide an in-

depth analysis of its performance under real-world conditions.

## 2. Materials and Methods

### 2.1 Materials

For the membrane preparation, 15 wt-% PVDF (Polyvinylidene Fluoride) (Sigma-Aldrich Chemie, Germany), 85 wt-% NMP (N-Methyl-2-Pyrrolidone), polydopamine (PDA) at concentrations of 0.5, 1, and 1.5 wt-% (Merck), and  $H_2SO_4$  (Merck) were used, with ethanol ( $C_2H_5OH$ ;  $\geq 99.0\%$ ) obtained from local suppliers serving as a solvent during the synthesis process. For the synthesis of the composite materials, sodium tungstate dihydrate ( $Na_2WO_4 \cdot 2H_2O$ ;  $\geq 99.0\%$ ) and zinc acetate dihydrate ( $Zn(CH_3COO)_2 \cdot 2H_2O$ ;  $\geq 99.0\%$ ) were used to prepare  $WO_3$  and ZnO, respectively, both sourced from Merck, Ltd., Singapore. Additionally, cetyltrimethylammonium bromide (CTAB;  $\geq 98.0\%$ ) was purchased from Sigma-Aldrich, Germany. The synthetic tetracycline wastewater was prepared by dissolving 25 mg of high-purity tetracycline powder ( $\geq 99\%$  purity) in 500 mL of deionized water to create a 50 mg/L tetracycline solution, stirred using a magnetic stirrer to ensure complete dissolution. The pH of the solution was adjusted to approximately pH 7.0 with hydrochloric acid (HCl) or sodium hydroxide (NaOH) as needed. This synthetic wastewater, simulating tetracycline contamination typically found in hospital effluents and agricultural runoff, was used in the subsequent treatment experiments.

### 2.2 Membranes Fabrication

ZnO nanoparticles were synthesized hydrothermally by mixing  $Zn(NO_3)_2 \cdot 6H_2O$  with NaOH, followed by heating to form crystalline ZnO. The product was filtered, washed, dried, and ground.  $WO_3$  was synthesized by dissolving  $Na_2WO_4 \cdot 2H_2O$  in water, adjusting the pH with  $HNO_3$ , and heating to form a yellow  $W^{6+}$  complex, followed by hydrothermal treatment, filtration, washing, drying, and calcination. Both materials were used for preparing the  $WO_3$ /ZnO photocatalyst. The  $WO_3$ /ZnO photocatalyst was prepared using a wet-impregnation method based on previous literature (Alsaiani et al., 2024). 1.4 g of  $WO_3$  and 0.014 g of ZnO were dispersed in 20 mL of ethanol, then subjected to ultrasonic agitation for 20 minutes. The suspension was stirred magnetically for 12–24 hours to promote interaction between  $WO_3$  and ZnO. After impregnation, the solid product was recovered by centrifugation or filtration, washed with ethanol and deionized water, dried at 60–80 °C, and ground to a uniform particle size for further characterization and evaluation of its adsorptive and photocatalytic properties. (TABLE 1)

**Table 1**

The formulations of the casting solutions utilized in membrane fabrication.

Membrane	NMP (wt%)	PVDF (wt%)	$WO_3$ /ZnO (wt%)
MV-01	85	13	-

Membrane	NMP (wt%)	PVDF (wt%)	WO <sub>3</sub> /ZnO (wt%)
MV-02	85	13	0,25
MV-03	85	13	0,75
MV-04	85	13	1,25

PVDF-WO<sub>3</sub>/ZnO membrane was successfully fabricated using the non-solvent induced phase inversion (NIPS) dry-wet technique. The membrane was modified by incorporating 1.25 wt% of WO<sub>3</sub>/ZnO nanoparticles (0.213 g), chosen as the optimal concentration, to assess the changes in the properties and performance of the modified membrane (Table 1). Initially, the photocatalyst nanoparticles were dispersed in NMP and sonicated for one hour to ensure uniform dispersion. Meanwhile, PVDF powder (13 wt%) was dissolved in NMP at 60°C for 20 minutes under continuous stirring at 1000 rpm, until a homogeneous solution was formed. Afterward, the photocatalyst nanoparticles were introduced into the casting solution, followed by 7 hours of stirring at 60°C and 24 hours of degassing. The blend was then cast onto a glass plate cooled with deionized water using a casting knife, and left for 24 hours to achieve a thickness of 0.15 mm. Subsequently, the cast membrane was immersed in a coagulation bath of deionized water for 24 hours, followed by air-drying overnight at room temperature.

### 2.3 Flux

Membrane filtration techniques rely heavily on flux as a primary measure of membrane performance. Flux refers to the volume of permeate that passes through a membrane's surface per unit of time, typically quantified in liters per square meter per hour (L·m<sup>-2</sup>·h<sup>-1</sup>). This parameter not only indicates the membrane's permeability but also serves as a critical factor in determining the efficiency of the filtration process. A higher flux generally means the membrane can handle larger volumes of water, which is advantageous for high-throughput operations such as wastewater treatment. However, flux can be influenced by several variables including the membrane material, pore structure, pressure applied, and the composition of the feed solution. The dynamics of flux are further complicated by factors like fouling, which can significantly alter flux over time (Field & Wu, 2022). In the present study, the focus was on examining the rate of permeate flow and the ability of the membrane to reject tetracycline (TC) and COD pollutants, using produced water as the feed. Initially, the membrane was compacted with demineralized water for 30 minutes under a transmembrane pressure of 5 bar, after which it was maintained at the same pressure with an effective membrane area of 1.26 × 10<sup>3</sup> m<sup>2</sup>. Permeate samples were taken every 30 minutes to monitor the flux behavior during the filtration process. The permeate water flux was quantified using the following Eq. (1)

$$J = \frac{\Delta V}{S \times \Delta t} \quad (1)$$

where J is the flux value (L·m<sup>-2</sup>·h<sup>-1</sup>); ΔV is the total volume collected permeate (L) during the operation time Δt (h), and S is the membrane effective area for filtration (m<sup>2</sup>).

This equation provides a quantitative way to assess the performance of various membrane systems and enables comparison between different materials and operational settings. Flux measurements also serve as an important tool for identifying fouling, as a notable drop in flux typically indicates the buildup of contaminants on the membrane's surface, leading to increased resistance. Fouling, whether from inorganic or organic matter, can cause partial or complete blockage of the membrane's pores, forming cake layers or contributing to internal fouling, which ultimately hinders the filtration process. Understanding how flux changes over time is crucial for optimizing membrane systems and improving their performance in real-world wastewater treatment applications (Jang et al., 2024).

### 2.4 Rejection Rate

In membrane filtration processes, rejection is a critical parameter that describes the ability of a membrane to retain contaminants while allowing water to pass through. It is usually quantified as a percentage, representing the difference in concentration of a solute between the feed and permeate solutions. A higher rejection percentage indicates a more effective membrane at preventing the passage of contaminants, such as salts, organic compounds, and microbial pathogens. The rejection capability of membranes depends on various factors, including their pore size, molecular sieving properties, and the charge interactions between the solutes and the membrane surface. Membranes, such as those used in reverse osmosis (RO) or nanofiltration (NF), typically rely on size exclusion and electrostatic repulsion to selectively block contaminants, making them suitable for advanced wastewater treatment. Nanofiltration membranes, for example, are particularly effective in removing multivalent ions and organic pollutants, which are commonly found in industrial effluents and wastewater streams (Ezugbe & Rathilal, 2020). The rejection rates were calculated using Eq. (2)

$$R_E = \left(1 - \frac{C_t}{C_o}\right) \times 100\% \quad (2)$$

Where R<sub>E</sub> is the pollutant removal efficiency (%), whereas C<sub>t</sub> and C<sub>o</sub> code as the contaminant level in permeate and feed, respectively.

In practice, rejection efficiency is often evaluated alongside flux, as both parameters are interrelated in determining overall membrane performance. While flux measures the amount of permeate passing through the membrane, rejection assesses how effectively contaminants are retained. A high flux rate combined with poor rejection is not ideal, as it could lead to the production of low-quality effluent. Conversely, a membrane with excellent rejection but low flux could significantly hinder operational efficiency. Rejection rates are typically measured by comparing the concentrations of specific solutes in the feed and permeate,

and are expressed as the percentage of removal. Over time, a decrease in rejection is often associated with fouling or membrane degradation, which can impede the filtration process and necessitate maintenance or replacement. Thus, rejection serves not only as a measure of selectivity but also as an indicator of long-term membrane performance in wastewater treatment applications (Hidalgo et al., 2023).

### 2.5 Porosity and Pore Size

The bentonite adsorption pretreatment was performed by introducing 1 gram of bentonite into 100 mL of produced water effluent in a beaker. The resulting suspension was continuously stirred using a magnetic stirrer for a duration of two hours. During the stirring process, aliquots were collected every 30 minutes for subsequent analysis. Following the mixing stage, the suspension was left undisturbed overnight to allow for sedimentation.

Membrane porosity and pore size are key structural parameters that influence fluid transport and separation efficiency in membrane filtration systems. Porosity represents the fraction of void spaces within the membrane matrix, which directly affects the ease with which water molecules traverse the membrane, while pore size determines the scale of particles or solutes that the membrane can retain or exclude. A membrane with higher porosity generally facilitates greater water permeability, yet the distribution and dimensions of pores must be carefully controlled to maintain adequate selectivity and minimize fouling. Similarly, the size and uniformity of pores dictate the rejection behavior and fouling tendency, as membranes with larger or uneven pores are more prone to clogging and reduced separation efficiency. Characterizing porosity and pore size therefore provides essential insight into membrane performance and helps guide the design and optimization of membranes for specific wastewater treatment applications (Wang et al., 2024). The membrane porosity was estimated using a very popular gravimetric method (Langone et al., 2021). Firstly, the membrane was carefully submerged in DI water compartment for 24 h, and was weighed afterward. After weighing, the wet membrane was dried in a vacuum oven with a temperature of 60 ° C for 24 h, and was weighed afterward as well. The apparent porosity was then calculated using Eq. (3). These comprehensive analytical methods offered valuable insights into the structural, chemical, and electrostatic attributes of the materials under investigation, thereby contributing significantly to the advancement of knowledge in this field.

$$\varepsilon = \frac{W_t - W_o}{\rho_w \times A \times \delta} \times 100\% \quad (3)$$

In the provided equation,  $\varepsilon$  represents the apparent porosity of the membrane, expressed as a percentage (%). The variables  $W_t$  and  $W_o$  denote the weights of the wet (g) and dry membranes (g), respectively. The symbol  $\rho_w$  corresponds to the density of pure water at room temperature, which is 0.997 g/cm<sup>3</sup>.  $A$  represents the contact

area of the membrane (cm<sup>2</sup>), while  $\delta$  signifies the thickness of the membrane (cm).

Furthermore, to ascertain the average pore size of the manufactured membranes, the Guerout-Elford-Ferry equation was employed, as delineated in Eq. (4). This equation offers an adequate mathematical framework for analyzing pore characteristics, thereby providing valuable insights into the structural properties of the membranes. Its utilization underscores the rigorous methodology adopted in this study to comprehensively evaluate the manufactured membranes, enhancing the credibility and significance of the findings presented.

$$r = \sqrt{\frac{8\eta\delta Q \times (2.9 - 1.75\varepsilon)}{\varepsilon \times A \times \Delta P}} \quad (4)$$

In the equation provided,  $\eta$  denotes the viscosity of pure water at room temperature, specified as  $8.9 \times 10^{-4} \text{ Pa} \cdot \text{s}$ .  $Q$  represents the volumetric flow rate of permeate water, measured in cubic meters per second (m<sup>3</sup>/s).  $\Delta P$  signifies the working pressure of the membrane system (Pa).

The mechanical properties of the membranes, including tensile strength and elongation at break, were evaluated using a universal testing machine (UTS, H001, China). To assess the hydrophilicity of the membranes, a contact angle meter (OCA25, Dataphysics Instruments, Germany) was employed to measure both the static contact angle and surface energy, providing crucial insights into their wetting behavior. The hydrophilicity was specifically evaluated by determining the contact angle between the surface of the WO<sub>3</sub>/ZnO-doped membrane and distilled water. Contact angle measurements were carried out with deionized (DI) water at 25°C, where droplets were placed on the membrane surface, and the contact angle was recorded after a 3-second interval. Additionally, the study extended to the water uptake capacity of the membranes, which was quantified using Equation (5). This thorough analysis offers a detailed understanding of both the mechanical strength and wetting properties of the membranes.

$$W_U = \frac{W_w - W_d}{W_d} \times 100\% \quad (5)$$

Where  $W_U$  showcases the membrane's water uptake (%),  $W_w$  and  $W_d$  show the weight of wet and dry membrane (g), respectively.

## 3. Results and Discussion

### 3.1 Flux Performance

Figure 1 presents the flux performance of various membranes tested under similar conditions. The data clearly show that the MV-0 membrane, containing 13% neat PVDF, exhibited the highest flux, followed by MV-2, which incorporates a 0.75% composite addition, resulting in a noticeable decrease in flux. The MV-3 membrane, with a 1.25% composite addition, showed a further reduction in flux, while the MV-1 membrane, incorporating 0.25%

composite, exhibited the smallest variation in flux compared to the others. While the MV-0 membrane demonstrates the highest initial flux, this does not necessarily indicate superior overall performance, as high flux is often achieved at the expense of selectivity and fouling resistance. In the field of membrane science, increased water permeability often correlates with reduced solute rejection or heightened fouling, highlighting the trade-off between flux and separation efficiency (Khan et al., 2025). Membranes MV-1 (0.25% composite), MV-2 (0.75% composite), and MV-3 (1.25% composite) exhibit this pattern: although their flux values are lower than MV-0, their flux decline over time is more gradual and stabilized, which suggests enhanced fouling resistance and sustained permeate flow over extended periods. Such stability is a characteristic feature of composite membranes, where the inclusion of hydrophilic and porous fillers boosts long-term performance by preserving consistent flux under operational conditions. These results underscore that although MV-0 provides the highest immediate flux, the composite membranes offer a more balanced combination of permeability and durability—critical attributes for practical wastewater treatment applications.

By incorporating functional fillers like  $WO_3/ZnO$  into the polymeric matrix, membranes can achieve a better balance between permeability and selectivity. The addition of composite materials often improves fouling resistance and solute rejection, as these nanomaterials modify the pore structure and surface properties to prevent the deposition of foulants and enhance contaminant retention. This trend is consistent with recent studies on advanced composite membranes, where optimized filler content enhanced antifouling properties and maintained flux while preserving separation efficiency (Popović et al., 2024). Therefore, despite their lower flux compared to PVDF neat, membranes MV-1, MV-2, and particularly MV-3 demonstrate more practical and reliable performance, with reduced flux decline and improved operational stability.

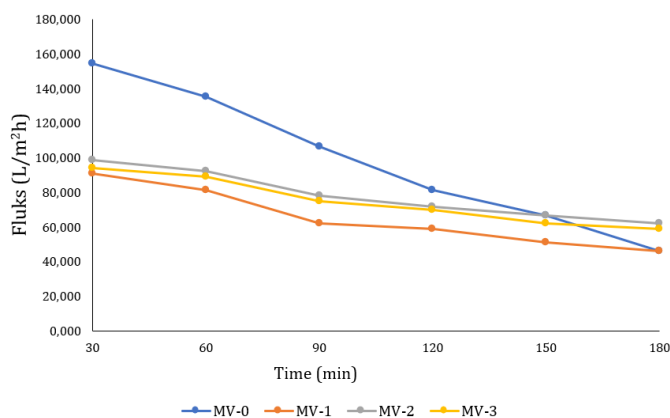


Figure 1. Permeate water flux of antibiotic wastewater

### 3.2 Pollutant Rejection Efficiency

Rejection efficiency is an essential performance indicator in membrane filtration, as it reflects the membrane's ability to prevent contaminants from passing through into the filtrate, thereby directly influencing the quality of treated water and ensuring compliance with discharge regulations (Hidalgo et al., 2023). In membrane technology, there is often an inherent trade-off between permeate flux and rejection efficiency. Typically, improvements in contaminant retention lead to a decrease in permeability, highlighting the delicate balance between selectivity and throughput that must be optimized, especially for wastewater treatment applications. According to Figure 2, the MV-3 membrane demonstrates the highest rejection efficiency for both pollutants, with a TC rejection rate of 98.28% and a COD rejection rate of 87.72%. The MV-2 membrane follows closely, achieving a TC rejection rate of 96.17% and a COD rejection rate of 75.94%. The MV-1 membrane shows 95.31% rejection for TC and 63.66% for COD. In contrast, the MV-0 membrane exhibits the lowest rejection efficiency, with a TC rejection rate of 94.94% and a COD rejection rate of 46.12%.

The increase in rejection efficiency observed with higher  $WO_3/ZnO$  content suggests that incorporating composite materials improves the membrane's ability to retain contaminants. In this study, membranes containing composite materials (MV-1, MV-2, and MV-3) show progressively higher rejection rates for both TC and COD compared to the pure PVDF neat membrane (MV-0). This pattern aligns with recent studies in membrane science, where nanocomposite polymer membranes exhibit enhanced selectivity due to the synergistic effects of fillers, which create more complex transport pathways for solutes, enhancing retention while reducing fouling (Khan et al., 2025). Furthermore, improvements in the membrane's structure—such as increased hydrophilicity and altered pore configurations resulting from the incorporation of nanoparticles—have been shown to boost contaminant rejection without significantly affecting permeate flux, provided the filler content is appropriately optimized (Binkadem, 2025). These findings substantiate the observation that increasing  $WO_3/ZnO$  loading enhances the interaction between the membrane matrix and pollutants, improving rejection efficiency, particularly for complex wastewater streams like antibiotic wastewater.

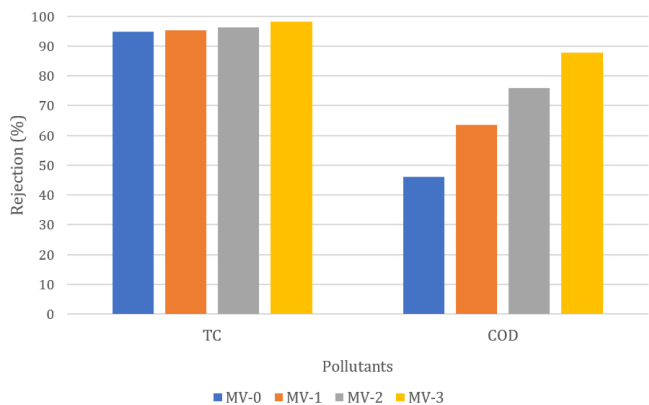


Figure 2. Pollutant rejection efficiency

### 3.3 Pore Properties of Membranes

The data presented in Table 2 provide valuable insights into the average porosity and pore radius of PVDF membranes, shedding light on the structural changes induced by the integration of photocatalysts. Figure 3 presents that the MV-0 membrane has the lowest porosity, recorded at 18.84%, while the MV-3 membrane demonstrates the highest porosity at 67.81%. The MV-1 membrane has a porosity of 49.59%, and MV-2 is positioned in between, with a porosity of 52.88%. While Figure 4 illustrates that MV-2 shows the largest average pore size 13.38 nm, followed by MV-3 that has an average pore size of 12.65 nm. MV-1 has an average pore size at 10.90 nm, while MV-0 exhibits the smallest average pore size at 10.74 nm. The addition of composite materials to PVDF membranes significantly affects their pore characteristics, influencing both porosity and pore size. As the data suggests, incorporating WO<sub>3</sub>/ZnO into the PVDF matrix led to an increase in both porosity and average pore size, particularly in membranes with higher concentrations (MV-2 and MV-3). This improvement contributes to better overall flux performance. However, this enhancement often comes with a trade-off, as larger pores can sometimes reduce the membrane’s ability to retain smaller pollutants. The relationship between pore size, porosity, and its effect on membrane performance underscores the importance of optimizing these factors to strike the best balance between permeability and rejection efficiency (Vo et al., 2024).

Table 1

Porosity and pore size of the membrane

Membrane	Porosity (%)	Average Pore Size (nm)
MV-0	18,84%	10.74 ± 0.01
MV-1	49,59%	10.90 ± 0.11
MV-2	52,88%	13.38 ± 0.05
MV-3	67,81%	12.65 ± 0.15

The integration of nanocomposite additives into polymeric membranes has been extensively studied, revealing their impact on structural features such as porosity and pore size, which directly influence filtration performance. Nanoparticles often facilitate the demixing process during phase inversion, resulting in a more porous membrane architecture and potentially larger pore channels compared to neat polymer membranes. While this structural modification can enhance water transport, it may also affect the membrane’s selectivity and rejection properties (Rouhollahi et al., 2024). Nanocomposite membranes that incorporate hydrophilic nanomaterials have shown an increase in both porosity and mean pore size compared to their unmodified counterparts, indicating that the interaction between nanofillers and the polymer matrix can create additional voids and facilitate pore formation during fabrication. Moreover, studies suggest that careful control of nanomaterial loading is essential, as excessive filler content can disrupt pore uniformity, leading to pore blockage or agglomeration, ultimately affecting the desired balance between permeability and selectivity (Nhlengethwa et al., 2024). These findings are consistent with observed trends in modified membranes, where higher nanocomposite loadings are linked to enhanced porosity but may result in altered pore size distributions that require optimization for optimal membrane performance.

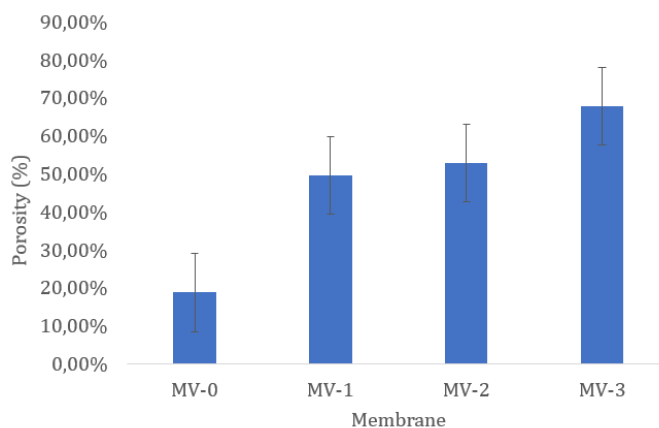
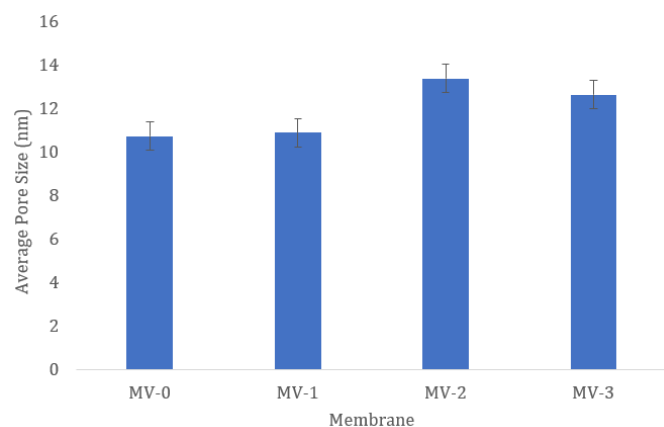


Figure 3. Porosity of the membrane



**Figure 4.** Average pore size of the membrane

#### 4. Conclusions

The performance of the membranes was assessed based on key parameters such as flux, pollutant rejection efficiency, and pore properties. Among the membranes tested, MV-3 (13% PVDF neat + 1.25%  $WO_3/ZnO$ ) demonstrated the highest flux performance, reaching approximately 90,000 L/m<sup>2</sup>.h, followed by MV-2 (13% PVDF neat + 0.75%  $WO_3/ZnO$ ) and MV-1 (13% PVDF neat + 0.25%  $WO_3/ZnO$ ). Regarding rejection efficiency, MV-3 also stood out with an impressive 98.28% rejection for tetracycline (TC) and 87.72% for COD. In terms of pore properties, MV-3 exhibited the highest porosity at 67.81%, while MV-2 had the largest average pore size of 13.38 nm. Although MV-3 delivered the best performance in rejection efficiency and porosity, it showed a slight decrease in flux compared to MV-2. Nonetheless, MV-3 remains the top-performing membrane overall, offering an optimal balance between high pollutant rejection and a moderate reduction in flux, making it the most suitable choice for antibiotic wastewater treatment applications.

#### Acknowledge

This project is financially supported by the grant of Publication Acceleration Research Diponegoro (RAP UNDIP) No. X/X/PP/X/2026. Special gratitude to the Institute for Research and Community Services, Diponegoro University (LPPM UNDIP) for the assistance during the completion of this project.

#### References

Alsaiari, N. S., Sultan Aljibori, H. S., Amari, A., Elboughdiri, N., El-Sabban, H. A., Diab, M. A., Ko, Y. G., Atamurotov, F., & Mahariq, I. (2024). Novel S-scheme  $WO_3/ZnO$ -modified g-C<sub>3</sub>N<sub>4</sub> heterojunction for optimizing norfloxacin photodegradation condition via DoE: Synthesis, characterization, and mechanism evaluation. *Journal of Water Process Engineering*, 67. <https://doi.org/10.1016/j.jwpe.2024.106276>

Binkadem, M. S. (2025). Polymeric composite membrane for brackish water treatment. *Journal of Saudi Chemical Society*, 29(5). <https://doi.org/10.1007/s44442-025-00032-y>

Carlet, J., Pulcini, C., & Piddock, L. J. V. (2014). Antibiotic resistance: A geopolitical issue. In *Clinical Microbiology and Infection* (Vol. 20, Issue 10, pp. 949–953). Blackwell Publishing Ltd. <https://doi.org/10.1111/1469-0691.12767>

Cifre-Herrando, M., Roselló-Márquez, G., Navarro-Gázquez, P. J., Muñoz-Portero, M. J., Blasco-Tamarit, E., & García-Antón, J. (2023). Characterization and Comparison of  $WO_3/WO_3-MoO_3$  and  $TiO_2/TiO_2-ZnO$  Nanostructures for Photoelectrocatalytic Degradation of the Pesticide Imazalil. *Nanomaterials*, 13(18). <https://doi.org/10.3390/nano13182584>

Ezugbe, E. O., & Rathilal, S. (2020). Membrane technologies in wastewater treatment: A review. In *Membranes* (Vol. 10, Issue 5). MDPI AG. <https://doi.org/10.3390/membranes10050089>

Field, R. W., & Wu, J. J. (2022). Permeate Flux in Ultrafiltration Processes—Understandings and Misunderstandings. *Membranes*, 12(2). <https://doi.org/10.3390/membranes12020187>

Frieri, M., Kumar, K., & Boutin, A. (2017). Antibiotic resistance. In *Journal of Infection and Public Health* (Vol. 10, Issue 4, pp. 369–378). Elsevier Ltd. <https://doi.org/10.1016/j.jiph.2016.08.007>

Gaur, N., Dutta, D., Singh, A., Dubey, R., & Kamboj, D. V. (2022). Recent advances in the elimination of persistent organic pollutants by photocatalysis. In *Frontiers in Environmental Science* (Vol. 10). Frontiers Media S.A. <https://doi.org/10.3389/fenvs.2022.872514>

Hidalgo, A. M., Gómez, M., Murcia, M. D., Gómez, E., León, G., & Alfaro, I. (2023). Prediction of Flux and Rejection Coefficients in the Removal of Emerging Pollutants Using a Nanofiltration Membrane. *Membranes*, 13(11). <https://doi.org/10.3390/membranes13110868>

Ibrahim, I., Elseman, A. M., Sadek, H., Eliwa, E. M., Abusaif, M. S., Kyriakos, P., Belessiotis, G. V., Mudgal, M. M., Abdelbasir, S. M., Elsayed, M. H., Mohamed, G. G., & Salama, T. M. (2025). Membrane-Based Photocatalytic and Electrocatalytic Systems: A Review. In *Catalysts*

- (Vol. 15, Issue 6). Multidisciplinary Digital Publishing Institute (MDPI).  
<https://doi.org/10.3390/catal15060528>
- Jang, H., Kang, S., & Kim, J. (2024). Identification of Membrane Fouling with Greywater Filtration by Porous Membranes: Combined Effect of Membrane Pore Size and Applied Pressure. *Membranes*, 14(2).  
<https://doi.org/10.3390/membranes14020046>
- Khan, I. A., Deen, K. M., Asselin, E., Yasir, M., Sadiq, R., & Ahmad, N. M. (2025). Boosting water flux and dye removal: Advanced composite membranes incorporating functionalized AC-PAA for wastewater treatment. *Journal of Industrial and Engineering Chemistry*, 145, 705–720.  
<https://doi.org/10.1016/j.jiec.2024.10.067>
- Kusworo, T. D., Soetrisantanto, D., Aryanti, N., Utomo, D. P., Qudratun, Tambunan, V. D., & Simanjuntak, N. R. (2018). Evaluation of Integrated modified nanohybrid polyethersulfone-ZnO membrane with single stage and double stage system for produced water treatment into clean water. *Journal of Water Process Engineering*, 23, 239–249.  
<https://doi.org/10.1016/j.jwpe.2018.04.002>
- Langone, M., Sabia, G., Petta, L., Zanetti, L., Leoni, P., & Basso, D. (2021). Evaluation of the aerobic biodegradability of process water produced by hydrothermal carbonization and inhibition effects on the heterotrophic biomass of an activated sludge system. *Journal of Environmental Management*, 299.  
<https://doi.org/10.1016/j.jenvman.2021.113561>
- Mallah, N. B., Shah, A. A., Pirzada, A. M., Ali, I., Khan, M. I., Jatoi, A. S., Ullman, J. L., & Mahar, R. B. (2024). Advanced Control Strategies of Membrane Fouling in Wastewater Treatment: A Review. In *Processes* (Vol. 12, Issue 12). Multidisciplinary Digital Publishing Institute (MDPI).  
<https://doi.org/10.3390/pr12122681>
- Mirwan, A., Indriyani, V., Novianty, Y., Yani, J. A., 36 Banjarbaru, K., & Selatan, K. (2017). *PEMBUATAN MEMBRAN ULTRAFILTRASI DARI POLIMER SELULOSA ASETAT DENGAN METODE INVERSI FASA*. 6(1), 12–17.  
<https://doi.org/10.20527/k.v6i1.4778>
- Nhlengethwa, S. T., Tshangana, C. S., Mamba, B. B., & Muleja, A. A. (2024). The Application of TiO<sub>2</sub>/ZrO<sub>2</sub>-Modified Nanocomposite PES Membrane for Improved Permeability of Textile Dye in Water. *Membranes*, 14(10).  
<https://doi.org/10.3390/membranes14100222>
- Popović, M., Morović, S., Kovačić, M., & Košutić, K. (2024). Pharmaceutical Removal with Photocatalytically Active Nanocomposite Membranes. In *Membranes* (Vol. 14, Issue 11). Multidisciplinary Digital Publishing Institute (MDPI).  
<https://doi.org/10.3390/membranes14110239>
- Rouhollahi, M., Mohammadi, T., Mohammadi, M., & Tofighy, M. A. (2024). Fabrication of nanocomposite membranes containing Ag/GO nanohybrid for phycoyanin concentration. *Scientific Reports*, 14(1).  
<https://doi.org/10.1038/s41598-024-73719-8>
- Sajjad, A. K. L., Sajjad, S., Iqbal, A., & Ryma, N. ul A. (2018). ZnO/WO<sub>3</sub> nanostructure as an efficient visible light catalyst. *Ceramics International*, 44(8), 9364–9371.  
<https://doi.org/10.1016/j.ceramint.2018.02.150>
- Vo, T. S., Lwin, K. M., & Kim, K. (2024). Recent developments of nano-enhanced composite membranes designed for water/wastewater purification—a review. In *Advanced Composites and Hybrid Materials* (Vol. 7, Issue 4). Springer Science and Business Media B.V.  
<https://doi.org/10.1007/s42114-024-00923-5>
- Wang, Y., Zhang, Y., Liang, L., Tu, F., Li, Z., Tang, X., Dai, L., & Li, L. (2024). Research Progress on Membrane Separation Technology for Oily Wastewater Treatment. In *Toxics* (Vol. 12, Issue 11). Multidisciplinary Digital Publishing Institute (MDPI).  
<https://doi.org/10.3390/toxics12110794>
- Yuju, S., Xiujuan, T., Dongsheng, S., Zhiruo, Z., & Meizhen, W. (2023). A review of tungsten trioxide (WO<sub>3</sub>)-based materials for antibiotics removal via photocatalysis. In *Ecotoxicology and Environmental Safety* (Vol. 259). Academic Press.  
<https://doi.org/10.1016/j.ecoenv.2023.114988>